Geometrically-Controlled Stimulus Responsive Surface Friction

Lin Han[*], Lifeng Wang[**], Jie Yin[**], Khek-Khiang Chia[***], Robert E. Cohen[***], Michael F. Rubner[*], Christine Ortiz[*] & Mary Boyce[** a)]

[*]*Department of Materials Science and Engineering,* [**]*Department of Mechanical Engineering, and* [***]*Department of Chemical Engineering, Massachusetts Institute of Technology, Cambridge, MA, 02139, U.S.A.*

Summary The pH-dependent mechanistic change in frictional mechanisms, and a × 5 – 6.5 fold change in friction coefficient μ, of layer-by-layer assembled poly(allylamine hydrochloride)/poly(acrylic acid) films were observed via lateral force microscopy and finite element analysis. This frictional response can be quantitatively controlled by the microscale anisotropic geometry, as demonstrated by the tube forest assembly, which undergoes ×2.5 – 3.5 fold change upon pH-stimulus.

Introduction Surfaces with tailored and well-controlled stimulus-responsive frictional properties hold great potential for an array of engineering and biomedical applications such as drug delivery, microfluidic devices, cell culture substrates and sensors [1]. To date, systems which exhibit stimulus-responsive surface friction, e.g., end-grafted polymer brushes [2] and cross-linked hydrogels [3], are largely controlled by molecular-level interactions. Such materials have been shown to undergo variations in the friction coefficient, μ, (the slope of the lateral versus applied normal force curve), up to an order of magnitude upon the application of stimuli such as temperature, pH, ionic strength and solvent. However, the controlled tunability of surface friction including sensitivity profile, range, temporal response still have yet to be fully realized and can be challenging through molecular-level design. Here, we explore the use of a fibrillar microscale geometry to control stimulus-responsive surface friction, which in addition to the contact area effect, results in a coupling between "inherent" material (molecular) responsiveness and induced deformation mechanisms associated with anisotropic shape and the heterogeneous spatial distribution of material.

Methods pH-dependent polyelectrolyte multilayers (PEM) were prepared via layer-by-layer assembly from poly(allylamine hydrochloride) (PAH, Sigma-Aldrich) and poly(acrylic acid) (PAA, Sigma-Aldrich, Fig. 1a) into anisotropic surface end-attached microtube forests and planar films (Fig. 1b), as described previously [4]. The pH-dependent dimensions of the film and tube forest were measured via atomic force microscopy (AFM) imaging and fluorescence microscopy [5]. For each sample, via improved wedge calibration [6], friction forces were quantified for at least 30 different scan lines over applied normal forces of 0 – 1.5 μN at 1 – 100 μm/s lateral displacement rates in aqueous solutions at both pH 2.0 (0.01 M HCl) and 5.5 (0.01 M NaCl) using a neutral, micro-spherical polystyrene tip (radius ~ 22.5 μm, nominal k ~ 14 N/m, Novascan) and a 3D Molecular Force Probe (Asylum Research). Friction coefficient μ was then calculated using least squares linear regression for each lateral displacement rate, pH and sample geometry (planar film versus tube forest). Finite element analysis (FEA) was conducted on both geometries to predict the friction behavior caused solely from the viscoelasticity of PAH/PAA at the applied normal force of ~ 1.0 μN by assuming both frictionless and frictional tip-sample surface contact (μ_S=0.1) with no overclosure for pH 2.0 and 5.0.

Results and Discussion The planar PAH/PAA PEM film exhibited a significantly higher friction in the ionically cross-linked contracted structure at pH 5.5 compared to the charged, hydrated and swollen structure at pH 2.0 [7]. At pH 5.5, the planar film exhibits dramatic relaxation in indentation (1 second for ~ 95% force relaxation) [5] due to extensive breaking/reformation of ionic cross-links. FEA simulations which assume frictionless tip-sample contact predict a friction coefficient of ~ 0.015 (10 μm/s lateral displacement rate), ~ 15% of the experimentally measured μ (0.114±0.005). Inclusion of a tip-sample surface friction coefficient, μ_S = 0.1 results in a net friction coefficient μ ~ 0.12, which is more closely approximates the experimental data. Hence, FEA simulations predict that the majority of the friction in this case originates from tip-surface interactions (~85% of μ) and a secondary contribution (~15% of μ) from viscoelasticity. The surface friction may originate from tip-sample adhesion-induced stretching of adsorbed polymer chains at the tip-sample interface, further suggested by the observed prominent "stick-slip" behavior, i.e., fluctuations of lateral force signals at ~ 1 μN normal force. In comparison, the planar film at pH 2.0 exhibits the absence of "stick-slip" in the lateral force versus displacement data, likely due to the presence of net positive charges ($-NH_3^+$ on PAH), the fluid-like hydration sheath surrounding these charges which can serve as lubricating layers to reduce surface friction with the neutral probe tip. In combination with the effect of less hydrophobicity and stronger electrostatic repulsion at pH 2.0, the friction response transitions from the stick-slip behavior at pH 5.5 to more of a lubricating behavior at pH 2.0. As a result, the friction forces are expected to be dominated by the viscoporoelastic effect due to the asymmetric stress distributions in the deformation zones at the back and front of the tip. FEA modeling confirms this mechanism and predicts a viscoelasticity-induced friction coefficient ~ 0.015 – 0.02 assuming frictionless contact, similar to the experimentally measured values of μ (0.017±0.001). As a result, a ~ 5 – 6.5 fold net increase in μ was observed for the planar film when changing pH from 2.0 to 5.5.

[a)] Corresponding author. Email: mcboyce@mit.edu.

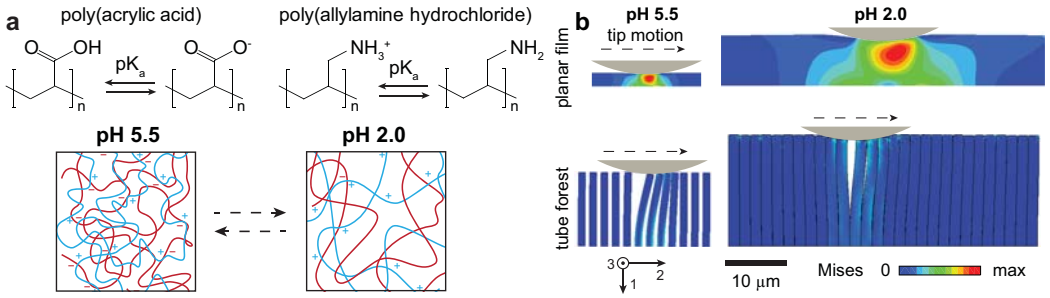

Fig. 1 *(a) pH-induced molecular-level interactions of PAH and PAA. (b) Von Mises stress distribution of the PAH/PAA film and tube forest during lateral scanning at both pH 2.0 and 5.5 under 1 μN applied normal force.*

Similar to the planar films, the PAH/PAA PEM tube forests also exhibited a significantly higher friction in the ionically cross-linked contracted structure at pH 5.5 than pH 2.0 [7]. At pH 5.5, the values of μ were slightly lower for the tube forests compared to the planar film (~ 0.10 – 0.12). Under these conditions, the tubes are initially (zero load) not in contact with each other (outer diameter, d_{out}, << tube center-to-center distance, w) resulting in "contact area splitting," a spatially heterogeneous material distribution and opportunity induced by the anisotropic geometry such as bending and buckling [5]. Hence, the normal and lateral forces were much lower for the tube forests at the same indentation depth similar to the previously reported nanoindentation experiment. FEA for the 10 μm/s lateral displacement rate predicts μ = 0.038 for frictionless contact and 0.095 for μ_S = 0.1, with the latter is similar to the experimental observation. The contribution of surface friction at pH 5.5 for the tube forest was reduced to ~ 60% of μ relative to the planar film (~ 85%) due to contact splitting and the fact that the stresses within the individual tubes were more distributed into the bulk of the material and also concentrated at the substrate. FEA simulations revealed that the other ~ 40% contribution to μ originated from an asymmetric distribution of PAH/PAA tube material around the center of the spherical tip, since the tubes ahead of the probe tip compared to behind the tip undergo different bending deformations. The rate dependence of PAH/PAA is found not to be a major contributor to its shear resistance for the tube forest at pH 5.5, similar to the case of the film. For the tube forest at pH 2.0, μ values (~ 0.025 – 0.045) were observed to the greater for the planar film (~ 0.015 – 0.024). At pH 2.0, swelling of the PAH/PAA network increased the tube cross-sectional area thereby resulting in inter-tube contacts and stress transfer between adjacent tubes. Hence, the tubes do not discretely bend and the indentation behavior is similar to that of the continuous film. At the same indentation depth, similar frictional forces were also observed for the film and tube forest. On the other hand, as the film experiences greater substrate compliance (H_{film}, 8.3 μm < $H_{tube,}$18 μm) [5] given the finite indentation depth, both the FEA model (Fig. 1b) and experiment shows higher indentation depth for the tube forest than the film under the same normal indentation force. Therefore, mainly owing to the smaller substrate constraints effect, the effective friction coefficient μ is higher for the tube forest relative to the film. In the absence of surface friction, FEA modeling also yields similar friction coefficient μ (~ 0.025 at 10 μm/s) to experimental observed values, suggesting surface friction contributes negligibly to the measured friction at pH 2.0, similar to the film. As a result of different shear deformation mechanisms for the tube forests compared to the film at both pHs, the increase in μ when changing pH from 2.0 to 5.5 is ~ 2.5 – 3.5 fold, which is lower than the planar film.

Conclusions One important observation emerging from this study is that the friction coefficient μ and underlying mechanisms of the polyelectrolyte system can be altered by both the solution pH (material stimulus) and the micro-scale geometry, such as tube forest versus the planar film. This result suggests stimulus-responsive polymers as a viable candidate for designing coatings with switchable frictional behavior upon external stimuli like temperature and pH. The responsiveness in frictional behavior can be further controlled by coupling with a variety of geometrical factors. For example, d_{out}, w, and aspect ratio of the tubes can be varied to induce friction behavior related to different deformation mechanisms, such as tube bending/buckling. In addition, when the substrate effect is not negligible (pH 2.0), a smaller thickness/height can lead to smaller indentation depth due to substrate constraints, and hence lower μ. All these factors can be utilized to design the polyelectrolyte multilayer systems with different frictional responses upon pH-stimulus that hold great potential for applications requiring quantitative control and switch of surface frictional properties.

References

[1] Bajpai A. K., Shukla S. K., Bhanu S., Kankane S., Responsive polymers in controlled drug delivery. *Prog. Polym. Sci.* **33**: 1088-1118, 2008.
[2] Nordgren N., Rutland M. W., Tunable nanolubrication between dual-responsive polyionic grafts. *Nano Lett.* **9**: 2984-2990, 2009.
[3] Chang D. P., Dolbow J. E., Zauscher S., Switchable friction of stimulus-responsive hydrogels. *Langmuir* **23**: 250-257, 2007.
[4] Chia K.-K., Rubner M. F., Cohen R. E., pH-Responsive reversibly swellable nanotube arrays. *Langmuir* **25**: 14044-14052, 2009.
[5] Han L., Wang L., Chia K.-K., Cohen R. E., Rubner M. F., Boyce M. C., Ortiz C., Geometrically controlled mechanically responsive polyelectrolyte tube arrays. *Adv. Mater.* **23**: 4667-4673, 2011.
[6] Han L., Dean D., Ortiz C., Grodzinsky A. J., Lateral nanomechanics of cartilage aggrecan macromolecules. *Biophys. J.* **92**: 1384-1398, 2007.
[7] Han L., Wang L., Yin J., Chia K.-K., Cohen R. E., Rubner M. F., Ortiz C., Boyce M. C., Geometrically controlled stimulus-responsive surface friction. In preparation.